Joseph Pierre Anderson[1]
School of Materials Engineering,
Purdue University,
701 West Stadium Avenue,
West Lafayette, IN 47907
e-mail: jpanderson@purdue.edu

Vignesh Vivekanandan
School of Materials Engineering,
Purdue University,
701 West Stadium Avenue,
West Lafayette, IN 47907
e-mail: vvivekan@purdue.edu

Peng Lin
School of Materials Engineering,
Purdue University,
701 West Stadium Avenue,
West Lafayette, IN 47907
e-mail: lin936@purdue.edu

Kyle Starkey
School of Materials Engineering,
Purdue University,
701 West Stadium Avenue,
West Lafayette, IN 47907
e-mail: starkeyk@purdue.edu

Yash Pachaury
School of Materials Engineering,
Purdue University,
701 West Stadium Avenue,
West Lafayette, IN 47907
e-mail: ypachaur@purdue.edu

Anter El-Azab
School of Materials Engineering,
Purdue University,
701 West Stadium Avenue,
West Lafayette, IN 47907
e-mail: aelazab@purdue.edu

Situating the Vector Density Approach Among Contemporary Continuum Theories of Dislocation Dynamics

For the past century, dislocations have been understood to be the carriers of plastic deformation in crystalline solids. However, their collective behavior is still poorly understood. Progress in understanding the collective behavior of dislocations has primarily come in one of two modes: the simulation of systems of interacting discrete dislocations and the treatment of density measures of varying complexity that are considered as continuum fields. A summary of contemporary models of continuum dislocation dynamics is presented. These include, in order of complexity, the two-dimensional statistical theory of dislocations, the field dislocation mechanics treating the total Kröner–Nye tensor, vector density approaches that treat geometrically necessary dislocations on each slip system of a crystal, and high-order theories that examine the effect of dislocation curvature and distribution over orientation. Each of theories contain common themes, including statistical closure of the kinetic dislocation transport equations and treatment of dislocation reactions such as junction formation. An emphasis is placed on how these common themes rely on closure relations obtained by analysis of discrete dislocation dynamics experiments. The outlook of these various continuum theories of dislocation motion is then discussed.
[DOI: 10.1115/1.4052066]

Keywords: constitutive relations, elastic behavior, mechanical behavior, microstructure property relationships, plastic behavior, principles of the micro-macro transition

1 Introduction

Almost 100 years have passed since dislocations were first asserted to be the carriers of plastic deformation in crystals [1–3], yet metal plasticity remains very much an open problem. Why is this the case? Many interesting phenomena regarding the plastic behavior of crystalline materials have their roots in the collective behavior of dislocations. However, the behavior of individual dislocations has long been well understood as they begin to interact they give rise to complex emergent behaviors.

Just as quantum theorists will never provide exact solutions to the many-body Schrödinger equation, our community will never provide exact solutions to many of the problems associated with the collective motion of dislocations. However, one strategy that is proving useful is the description of the dislocation field in a crystal using measures of increasing generality in the hopes of distilling relations between particular behaviors and the dislocation structure at a particular length scale. The purpose of this article is to present several such efforts to describe the dislocation system. In doing so, we will encounter problems whose solutions are within the grasp of these various theories as well as some horizons of dislocation dynamics, which remain puzzling.

Presented here are four models that describe the evolution of dislocation densities in a crystal, which is four models of continuum dislocation dynamics (CDD). They differ widely in their approaches, but all are instructive toward building a cohesive picture of the collective behavior of dislocations. In this presentation, we hope to situate our own work on the vector density approach to dislocation dynamics in the present field of CDD frameworks. In addition, we will examine the strengths and limits of each model, and try to understand how each can inform the other in advancing our community's understanding of plastic behavior.

However, models describing the evolution of various dislocation density fields by no means have an exclusive claim to supremacy in plasticity theory. Rather continuum approaches enjoy a healthy camaraderie with theories of discrete dislocation dynamics (DDD) [4–8], which treat the evolution of a collection of discrete lines in a crystal. DDD calculations show promise in revealing information about the self-organization of dislocations, where the effect of short-

[1]Corresponding author.

Contributed by the Materials Division of ASME for publication in the Journal of Engineering Materials and Technology. Manuscript received March 8, 2021; final manuscript received July 27, 2021; published online August 30, 2021. Assoc. Editor: David Field.

range interactions such as dislocation reactions has been found to be significant [9–11]. As the field has progressed, novel phenomenological rules for these interactions and for the mobility of dislocations have been developed, which are typically informed from lower scale atomistic calculations [6,12–14]. Many novel situations benefit from the specificity of considering the positions of individual dislocation lines. These include studies of strain bursts and avalanche dynamics in finite crystals [15–19] and interactions of glide dislocations with other material defects such as stacking fault tetrahedra, prismatic loops, voids, and secondary phases [20–22]. However, the downfall of these discrete models is a computational complexity wall produced by the multiplication of dislocations in a system as strain increases. While significant efforts have been made in improving the computational efficiency of DDD using novel computational methods, e.g., multipole method for long-range stress calculations [4,23], subcycling time integration schemes [24,25], GPU-accelerated schemes [26], and fast Fourier transform-based schemes [27]–computations become prohibitively expensive beyond ~1% strain. Even if this wall was not an issue, the kinematics of discrete lines at such finite deformations begin to break down the assumptions on which the entire method is based [28,29]. As the field of discrete dislocation dynamics advances and suitable boundary conditions are devised to compare DDD with the mechanical environment of CDD [30], data gathered from DDD experiments help to inform CDD models. In addition to an overview of CDD methods, we hope to give a glimpse into how discrete simulation data are used to inform these continuum models of dislocation dynamics.

With all this in mind, we outline this article as follows. We summarize the two-dimensional (2D) models pioneered by Groma, Zaiser, and coworkers in Sec. 2; the field dislocation mechanics (FDM) of Acharya and coworkers in Sec. 3; the vector density approach to CDD that we, the present authors, commonly employ in Sec. 4; and finally, the most general kinematics of curved dislocations developed by Hochrainer and associates in Sec. 5. We hope to illustrate how all of these inform, extend, or generalize each other, as well as how each is in turn informed by DDD experiments.

2 Two-Dimensional Theories

The first forays into statistical considerations of dislocations were motivated by interpreting x-ray diffraction line broadening in terms of the dislocation content of a crystal [31–33]. In this line of thinking, there arose a statistical model of straight, parallel edge dislocations to deal more precisely with the x-ray line broadening problem [34], based on the Born–Bogoliubov–Green–Yvon–Kirkwood (BBGKY) density hierarchy description of particle systems [35–37]. The analogy to particle systems appears by considering these perfectly straight and parallel dislocations of Burgers vector $\hat{x}$ to be two species of particles located in a plane (which we will refer to as the xy-plane). These two species (positive and negative) arise from the tangent vector of the dislocation lying along $+\hat{z}$ or $-\hat{z}$. The signed dislocation density measure, if chosen as the random variable of consideration, would cause cancellation in some scenarios. As a result, the density field is often considered to be dependent on the orientation space $\mathbb{T}$, which in this case is simply $\mathbb{T} := -1,\ +1$. The statistical process of defining the continuum fields begins with the discrete dislocation system, having density:

$$\rho_{\pm}^{(D)}(\boldsymbol{r}) = \sum_{i=1}^{N_{\pm}} \delta(\boldsymbol{r} - \boldsymbol{r}_i) \tag{1}$$

where $\boldsymbol{r}_i$ is the location of the ith of $N_{\pm}$ positive or negative dislocations, respectively. Considering the average behavior of these discrete densities over many such possible configurations results in a hierarchy of continuum densities (compared with BBGKY hierarchies):

$$\rho_{\pm}(\boldsymbol{r}) := \left\langle \rho_{\pm}^{(D)}(\boldsymbol{r}) \right\rangle \tag{2}$$

$$\rho_{++}(\boldsymbol{r}, \boldsymbol{r}') := \left\langle \rho_{+}^{(D)}(\boldsymbol{r}) \rho_{+}^{(D)}(\boldsymbol{r}') \right\rangle \tag{3}$$

$$\rho_{+-}(\boldsymbol{r}, \boldsymbol{r}') = \rho_{-+}(\boldsymbol{r}', \boldsymbol{r}) := \left\langle \rho_{+}^{(D)}(\boldsymbol{r}) \rho_{-}^{(D)}(\boldsymbol{r}') \right\rangle \tag{4}$$

$$\rho_{--}(\boldsymbol{r}, \boldsymbol{r}') := \left\langle \rho_{-}^{(D)}(\boldsymbol{r}) \rho_{-}^{(D)}(\boldsymbol{r}') \right\rangle \tag{5}$$

A straightforward averaging of the equations of motion of the individual dislocations results in the following evolution equations for the single-point densities:

$$\partial_t \rho_+ = -M_0 b\, \partial_x \Big[\rho_+(\boldsymbol{r}) \tau_{\text{ext}} + \int \{ \rho_{++}(\boldsymbol{r}, \boldsymbol{r}') - \rho_{+-}(\boldsymbol{r}, \boldsymbol{r}') \} \tau_{\text{int}}(\boldsymbol{r} - \boldsymbol{r}')\, d^2\boldsymbol{r}' \Big] \tag{6}$$

$$\partial_t \rho_- = +M_0 b\, \partial_x \Big[\rho_-(\boldsymbol{r}) \tau_{\text{ext}} - \int \{ \rho_{--}(\boldsymbol{r}, \boldsymbol{r}') - \rho_{-+}(\boldsymbol{r}, \boldsymbol{r}') \} \tau_{\text{int}}(\boldsymbol{r} - \boldsymbol{r}')\, d^2\boldsymbol{r}' \Big] \tag{7}$$

where M_0 is a mobility constant, b is the length of the Burgers vector, τ_{ext} is the externally applied shear stress, and τ_{int} is the kernel of the interaction stress between two edge dislocations. These equations are not usable in their present form without a closure relation for the two-point densities. It is a common practice in density hierarchy approaches to factor out the dependence on the single-point densities [38], expressing the two-point densities in the following manner:

$$\rho_{s_1 s_2}(\boldsymbol{r}, \boldsymbol{r}') := \rho_{s_1}(\boldsymbol{r}) \rho_{s_2}(\boldsymbol{r}') \big(1 + d_{s_1 s_2}(\boldsymbol{r} - \boldsymbol{r}') \big) \tag{8}$$

where s_1 and s_2 are the desired species (positive or negative) of dislocation to be represented, and $d_{s_1 s_2}$ are the dislocation correlation functions. By assuming that the correlation functions decay fast compared to the lengths on which $\rho_{\pm}$ varies, all correlation effects can be expressed in terms of local field variables at $\boldsymbol{r}$ [39–42]. This approximation allows the evolution equations for the total dislocation density $\rho(x, y) := \rho_+ + \rho_-$ and the geometrically necessary dislocation (GND) density $\kappa(x, y) := \rho_+ - \rho_-$ to be expressed as follows [43]

$$\partial_t \rho = -M_0 b \partial_x [\kappa\, (\tau_{\text{mf}} - \tau_{\text{b}}) - \rho\ \tau_{\text{d}}] \tag{9}$$

$$\partial_t \kappa = -M_0 b \partial_x \left[\rho \left(\tau_{\text{mf}} - \tau_{\text{b}} - \tau_{\text{f}} \left(1 - \left(\frac{\kappa}{\rho} \right)^2 \right) \right) - \kappa\ \tau_{\text{d}} \right] \tag{10}$$

where the dislocations evolve under the influence of the mean-field stress τ_{mf}, as well as emergent effective stresses: the back stress τ_{b}, the flow stress τ_{f}, and the diffusion stress τ_{d}. These quantities are defined as follows:

$$\tau_{\text{mf}} = \tau_{\text{ext}} + \int \kappa(\boldsymbol{r}') \tau_{\text{int}} d^2\boldsymbol{r}' \tag{11}$$

$$\tau_{\text{b}} = \frac{D}{\rho} \partial_x \kappa \tag{12}$$

$$\tau_{\text{f}} = \alpha \sqrt{\rho} \tag{13}$$

$$\tau_{\text{d}} = \frac{A}{\rho} \partial_x \rho \tag{14}$$

where D, A, and α are dimensionless constants. More specifically, they are integral moments of the correlation functions [42]. The effects of these effective stresses are clearly seen in the behavior of Eqs. (9) and (10) in the limit of $|\kappa| \ll \rho$, that is, a nearly homogeneous system. In such a case, terms quadratic in $|\kappa|/\rho$ are neglected: the diffusion stress τ_d leads to diffusion in the evolution of ρ, the back stress τ_b partially negates the mean-field stress and is related to pile-ups of dislocations, while the flow stress τ_f represents the dynamic breaking and forming of dipoles and results in a Taylor-type flow stress. From the outset, these correlation-dependent terms have been calibrated against 2D DDD simulations. These correlation functions began to be calculated as measures of the dislocation microstructure [44,45] and were then co-opted for their kinetic relevance to these effective stresses [37,40].

In recent years, Groma et al. have stressed that the equations of motion have a phase-field-type structure [46]. That is to say, they can be expressed as gradients of chemical potentials that are, in turn, variational derivatives of a potential function with respect to a state variable. That is, these evolution equations can be expressed as follows for weakly polarized systems ($\kappa \ll \rho$) [43]:

$$\partial_t \begin{pmatrix} \rho \\ \kappa \end{pmatrix} = \left[\partial_x \begin{pmatrix} \zeta(\delta P/\delta \rho) & \delta P/\delta \kappa \\ \delta P/\delta \kappa & \zeta(\delta P/\delta \rho) \end{pmatrix} \right] \begin{pmatrix} \rho \\ \kappa \end{pmatrix} \tag{15}$$

where a so-called plastic potential P is introduced, having the form:

$$P[\chi, \kappa, \rho] := P_{\mathrm{mf}}[\chi, \kappa] + P_{\mathrm{corr}}[\rho, \kappa] \tag{16}$$

$$P_{\mathrm{mf}}[\chi, \kappa] := \int -\frac{1-\nu}{4\mu}(\nabla^2 \chi)^2 + b\chi\, \partial_y \kappa \; d^2\boldsymbol{r} \tag{17}$$

$$P_{\mathrm{corr}}[\rho, \kappa] := Gb^2 \int A\rho \ln\left(\frac{\rho}{\rho_0}\right) + \frac{D}{2}\frac{\kappa^2}{\rho} \; d^2\boldsymbol{r} \tag{18}$$

In the aforementioned expressions, χ represents the Airy stress potential; minimization of P_{mf} with respect to χ gives $\tau_{\mathrm{mf}} := \partial_x \partial_y \chi$ in terms of κ.

The only term in the plastic potential that does not naturally appear in the elastic energy functional is a portion of the natural logarithm term, which produces the diffusion stress [39]. In the energy functional, this logarithm represents the self-energy of the dislocation line and is free from any correlation dependence. However, in the plastic potential (Eq. (18)), an integral of the correlation (A) appears.

While this system may seem simplistic on the surface, it has many lessons to teach about the role of statistical considerations in the collective motion of dislocations. In the more than 20 years of comparative studies with DDD experiments, many nuances of the statistical description have been discovered. These comparisons have shown, for example, the aforementioned emergence of correlation-dependent effective stresses [37,40], a discrepancy between the mobility of the discrete dislocations and dislocation density fields [47], and a dependence of the effective stresses on density resolution and on the local stress field [48]. Moreover, it has shed valuable light on the role of the collective motion of dislocations in plasticity at inclusion interfaces [49], the behavior of dislocation pile-ups [50], and the emergence of dislocation patterns [42,43,51]. A recent stochastic implementation has shown useful in describing problems related to intermittent dislocation flow [43,51,52]. This simplified continuum model seems to be a veritable fount of interesting behavior, and as such, it will help inform directions of inquiry for three-dimensional (3D) continuum methods, to which we now turn our attention.

3 Field Dislocation Mechanics

Since dislocations were identified as the carriers of permanent deformation in a solid, there has been a considerable interest in the internal mechanical fields they produce. In the bulk, the stress field is a combination of the internal stress, which depends on the spatial distribution of dislocations, and the external stress, which arises from the applied boundary conditions. As a result, the evolution of the internal dislocation microstructure should be considered to accurately predict the mechanical response of a crystal. The classical theory, the elastic theory of continuously distributed dislocations (ECDD) [53], accomplishes this by means of the Kröner–Nye dislocation density tensor $\boldsymbol{\alpha}$ [54]. This tensor represents the geometrically necessary dislocations of each unique Burgers vector by considering:

$$\boldsymbol{\alpha}(\boldsymbol{r}) := \sum_{\gamma} \rho_{\mathrm{GND}}^{[\gamma]}(\boldsymbol{r})\left(\boldsymbol{\xi}^{[\gamma]}(\boldsymbol{r}) \otimes \boldsymbol{b}^{[\gamma]}\right) \tag{19}$$

where $\rho_{\mathrm{GND}}^{[\gamma]}(\boldsymbol{r})$ is the total line length of GNDs at $\boldsymbol{r}$ due to slip system γ, $\boldsymbol{\xi}$ is the net direction of the GNDs, and $\boldsymbol{b}^{[\gamma]}$ is the Burgers vector of that slip system. Due to the summation across slip systems, some information regarding the GND content is lost. Some theories of plasticity have treated this problem by assuming the underlying dislocations to be pure edge and screw type. Still, there are several theories which directly treat the evolution of $\boldsymbol{\alpha}$ (see the works of Gurtin [55]; Shizawa and Zbib [56–58]; and Acharya and Roy [59,60]). We will focus on the current form of FDM due to Acharya [59]. The geometrically linear version of FDM consists of the following basic equations [61]:

$$\nabla \times \boldsymbol{\beta}^{\mathrm{P}} = -\boldsymbol{\alpha} \tag{20}$$

$$\boldsymbol{\beta}_{\parallel}^{\mathrm{P}} = \tilde{\boldsymbol{\beta}}_{\parallel}^{\mathrm{P}} \tag{21}$$

$$\boldsymbol{\varepsilon} := \frac{1}{2}\left(\boldsymbol{\beta} + \boldsymbol{\beta}^T\right), \quad \boldsymbol{\varepsilon}^{\mathrm{P}} := \frac{1}{2}\left(\boldsymbol{\beta}^{\mathrm{P}} + (\boldsymbol{\beta}^{\mathrm{P}})^T\right) \tag{22}$$

$$\boldsymbol{\sigma} = \mathbb{C}(\boldsymbol{\varepsilon} - \boldsymbol{\varepsilon}^{\mathrm{P}}), \qquad \nabla \cdot \boldsymbol{\sigma} = 0 \tag{23}$$

$$\partial_t \boldsymbol{\alpha} = -\nabla \times (\boldsymbol{\alpha} \times \boldsymbol{V}) + \boldsymbol{s} \tag{24}$$

$$\partial_t \tilde{\boldsymbol{\beta}}^{\mathrm{P}} = \boldsymbol{\alpha} \times \boldsymbol{V} \tag{25}$$

$\boldsymbol{\beta}$ is the displacement gradient, and $\tilde{\boldsymbol{\beta}}^{\mathrm{P}}$ and $\boldsymbol{\beta}^{\mathrm{P}}$ are the slip and plastic distortions, respectively. $\tilde{\boldsymbol{\beta}}_{\parallel}^{\mathrm{P}}$ and $\boldsymbol{\beta}_{\parallel}^{\mathrm{P}}$ are their compatible parts, $\boldsymbol{\sigma}$ is the stress tensor, and $\mathbb{C}$ is the fourth-order elastic modulus tensor. $\boldsymbol{V}$ is the dislocation velocity tensor, and $\boldsymbol{s}$ is a dislocation source term. The plastic distortion is decomposed into an incompatible part and a compatible part, which are determined by Eqs. (20) and (21), respectively. Equations (22) and (23) are the standard stress constitutive equation and equilibrium equation, respectively. Equation (24) depicts the evolution of dislocation density tensor, and its derivation is based on localizing an integral balance law for the Burgers vector of dislocations that thread an arbitrary surface. Equation (25) represents the evolution of the slip distortion due to the motion of dislocations.

The novel contribution of FDM is Eq. (21). It should be pointed out that the decomposition of the plastic distortion into a compatible and incompatible part is an important feature of FDM compared with other continuum dislocation approaches. In ECDD [53], only Eqs. (20), (22), and (23) are considered, and they predict the internal stress field when the dislocation density field is known in a configuration. Acharya [59] showed that the equations of ECDD are inadequate for the unique determination of the physical displacement field due to the gauge invariance of Eq. (20). In fact, the compatible part of plastic distortion depends on the history of dislocation evolution, so Eqs. (24) and (25) are required to determine the physical displacement. These evolution equations for the dislocation density tensor is motivated by the work of Mura [62] and Kosevich [63]. However, the treatment of the plastic distortion and dislocation flux with the added nuance of the

compatibility condition (21) distinguishes FDM from these earlier models.

In the first version of FDM, the nonuniqueness of the plastic distortion field was rectified by using a certain gauge specification amounting to fixing the weak form of the curl equation (20) with respect to an orthogonality projection [59]. This rather abstract constraint on the curl equation was later replaced [64] with the specification of an additional position vector field. It has also shown in a recent work [65] that the decomposition of plastic distortion as in FDM can also help in reducing the numerical errors compared with direct time integration of Eq. (25).

To close the FDM theory, a theoretical guideline to deriving constitutive closure, driving forces for the dislocation velocity, and dislocation nucleation rates were derived from the standard continuum mechanics formulations of thermodynamics [64,66]. These studies showed the driving force is of a similar form to the Peach–Koehler force on a single dislocation from the total local stress. A phenomenological mesoscopic field dislocation mechanics (PMFDM) was also developed [60,61], which results from coarse graining of the FDM equations in both space and time. By closing these equations using free-energy arguments, PMFDM is able to study practical problems of mesoscopic and macroscopic plasticity with linkage to the theory of continuously distributed dislocations.

Field dislocation mechanics theory has been analytically shown to possess the capability of predicting fundamental features of dislocation plasticity in solids, for example, it predicts the stress field of edge and screw dislocations in an isotropic medium [59]. Numerical schemes of FDM has also been implemented to study more complicated and practical problems, for example, size effects [60], dislocation walls [67], the effect of passivation and grain boundaries [68], as well as dislocation microstructures [69,70].

The theory of FDM is more often compared to crystal plasticity models than to DDD experiments [68,69]. However, we include it among the discussion of continuum models of dislocation dynamics because not only of its important link to the classical theories of distributed dislocations but also of its importance to solutions of the mechanical fields in continuum dislocation dynamics. In fact, solutions for the mechanical fields based on the Kröner–Nye tensor $\boldsymbol{\alpha}$ are beginning to be used even in discrete dislocation mechanics [27,71] due to a lower computational complexity relative to the number of dislocation segments considered. However, the mechanical fields due to $\boldsymbol{\alpha}$ are analogous to the mean-field stress of Eq. (11), and additional statistical effects would need to be considered [72] in a more complete theory.

Because the total dislocation density tensor $\boldsymbol{\alpha}$ is used in the dislocation evolution equation, the physical meaning of the associated dislocation velocity $\boldsymbol{V}$ is not straightforward [73]. Moreover, it seems to be difficult to consider dislocation junction reactions between different slip systems when the evolution equation is only based on the total dislocation density tensor. The source terms in Eq. (24) are included to describe dislocation nucleation [66], but junction reactions would require more nuance.

4 Vector–Density Based Theories

The representation that needs the least information to properly resolve the kinematics of curved dislocation lines is one that treats dislocations as vector densities and distinguishes between densities on different slip systems [73]. This vector density approach has also been called the theory of purely geometrically necessary dislocations [74,75]. Its creation was motivated by a desire to study the onset of dislocation patterning [76] and the emergence of lattice misorientations as subgrains begin to form Ref. [77]. In considering the basis of the vector density approach, it is helpful to consider the problem of discrete dislocation dynamics as the evolution of a collection of line objects $\mathcal{L}^{[\alpha]}$ corresponding to the dislocation objects on each slip system α. These line objects can be recast as discrete densities analogously to the 2D case (Eq. (1)):

$$\boldsymbol{\rho}^{(D)}_{\mathcal{L}^{[\alpha]}}(\boldsymbol{r}) = \int_{\mathcal{L}^{[\alpha]}} \delta(\boldsymbol{r} - \boldsymbol{r}_l)\, d\boldsymbol{l} \tag{26}$$

where $d\boldsymbol{l}$ includes the tangent direction of the line object at $\boldsymbol{r}_l$. The smooth vector density field is then obtained by means of any suitable ensemble average such that

$$\boldsymbol{\rho}^{[\alpha]}(\boldsymbol{r}) = \left\langle \boldsymbol{\rho}^{(D)}_{\mathcal{L}^{[\alpha]}}(\boldsymbol{r}) \right\rangle \tag{27}$$

$$\left| \hat{\boldsymbol{a}} \cdot \boldsymbol{\rho}^{[\alpha]}(\boldsymbol{r}) \right| = \left\langle \left| \hat{\boldsymbol{a}} \cdot \boldsymbol{\rho}^{(D)}_{\mathcal{L}^{[\alpha]}}(\boldsymbol{r}) \right| \right\rangle \tag{28}$$

for any arbitrary constant vector $\hat{\boldsymbol{a}}$. The second requirement (28) is referred to as the line bundle assumption [78] and is a formal definition of how the theory considers only GNDs. This assumption implies that all the underlying discrete dislocations considered by the smooth vector density $\boldsymbol{\rho}^{[\alpha]}$ have tangent vector parallel to the vector density. As a result, the ensemble average operation in Eq. (27) has no cancellation (which would produce statistically stored dislocations), and the magnitude of the vector density is equal to the total dislocation line density at each point. In such a regime, the streamlines of the density field (Fig. 1) can be considered as the approximate positions of the underlying discrete dislocations. The accuracy of this approximate position is relative to the resolution on which the vector–density is evaluated: at distances shorter than the chosen resolution, interactions must be considered in a statistical manner. The behavior of these short-range interactions has been seen to be strongly dependent on the chosen length scale used to describe the density fields as the line bundle assumption breaks down above the average dislocation spacing [78].

By means of the line-bundle assumption, the transport equation can be expressed as follows [75,79,80]:

$$\partial_t \boldsymbol{\rho}^{[\alpha]} = \nabla \times \left\langle \boldsymbol{v}^{[\alpha]} \times \boldsymbol{\rho}^{[\alpha]} \right\rangle + \dot{\boldsymbol{\rho}}^{[\alpha]}_{\text{source}} - \dot{\boldsymbol{\rho}}^{[\alpha]}_{\text{sink}} \tag{29}$$

where $\boldsymbol{v}^{[\alpha]}$ is the velocity of the line object $\mathcal{L}^{[\alpha]}$ and $\dot{\boldsymbol{\rho}}^{[\alpha]}_{\text{source}}$, $\dot{\boldsymbol{\rho}}^{[\alpha]}_{\text{sink}}$ can be used to transfer dislocation densities between slip systems as in the case of dislocation reactions or cross-slip. In the self-consistent field formulation (i.e., neglecting correlation effects), the slip rate

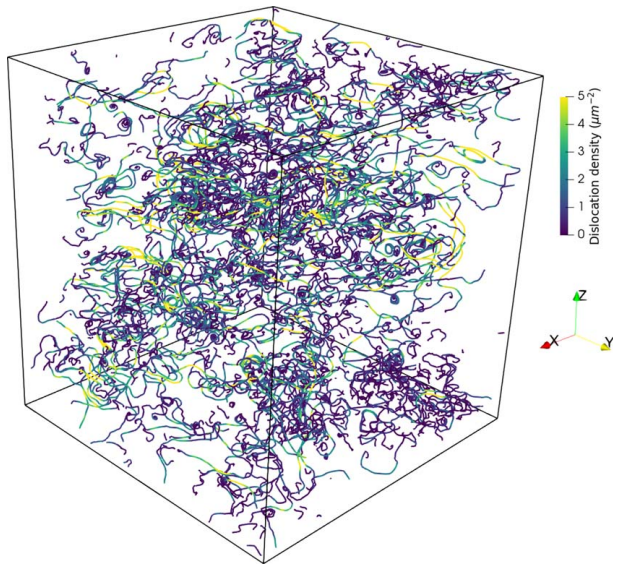

Fig. 1 Streamlines of the density field of dislocations on a single slip system in the line-bundle regime. Taken from a typical vector density-based CDD simulation of a (5 × 5 × 5.3) μm^3 crystal volume of steel strained to 0.6%. These streamlines represent the approximate position of the underlying discrete dislocation objects.

vector $\langle \boldsymbol{v}^{[\alpha]} \times \boldsymbol{\rho}^{[\alpha]} \rangle$ is expressed by means of the Peach–Koehler force:

$$\left\langle \boldsymbol{v}^{[\alpha]} \times \boldsymbol{\rho}^{[\alpha]} \right\rangle = \left\langle \boldsymbol{v}^{[\alpha]} \right\langle \times \boldsymbol{\rho}^{[\alpha]} = \left(Mb\, \tau^{[\alpha]}\, \hat{\boldsymbol{v}}^{[\alpha]} \right) \times \boldsymbol{\rho}^{[\alpha]} \tag{30}$$

where M is a mobility constant, b is the length of the Burgers vector, $\tau^{[\alpha]}$ is the resolved shear stress on slip system α, and $\hat{\boldsymbol{v}} := \hat{\boldsymbol{n}}^{[\alpha]} \times (\boldsymbol{\rho}^{[\alpha]}/|\boldsymbol{\rho}^{[\alpha]}|)$ is the direction normal to the slip plane and the dislocation density vector.

The line-bundle assumption not only produces a simplified transport equation (29) but also allows treatment of dislocation reactions by a conventional reaction rate-type theory [81]. In this construction, two reacting slip systems β, γ produce a product density on slip system α:

$$\dot{\boldsymbol{\rho}}^{[\alpha]}_{\text{source}} = \boldsymbol{\rho}^{[\beta]} \cdot \boldsymbol{R}^{[\beta,\gamma]\to[\alpha]} \cdot \boldsymbol{\rho}^{[\gamma]} \tag{31}$$

allowing dislocations to leave the slip system by means of their respective sink terms. The rate constant $\boldsymbol{R}^{[\beta,\gamma]\to[\alpha]}$ for this process is defined based on the relative velocities of dislocations in the two reagent slip systems and a length-scale parameter that characterizes the effective junction length [81]. The reaction rate takes into consideration the effect of orientation of the reacting dislocations based on an energy criterion to decide whether the reaction is feasible. This is possible because the orientation of the underlying dislocations is well defined due to the line-bundle assumption. These rate constants can then be calibrated against junction data from DDD experiments [82,83].

Moreover, while Eq. (30) allows for the consideration the transport equation in a self-consistent field context, the dislocation correlation functions of the vector density system has recently been shown [78] to have a simple form, whereby the two-point density may be expressed (compared with Eq. (8)):

$$\left\langle \rho_i^{(D)[\alpha]}(\boldsymbol{r}) \rho_j^{(D)[\beta]}(\boldsymbol{r}') \right\rangle = \rho_i^{[\alpha]}(\boldsymbol{r}) \rho_j^{[\beta]}(\boldsymbol{r}') \left(1 + d^{(i,j)[\alpha,\beta]}(\boldsymbol{r} - \boldsymbol{r}') \right) \tag{32}$$

where $\rho_i^{(D)[\alpha]}(\boldsymbol{r})$ represents the ith component of $\boldsymbol{\rho}^{(D)}_{\mathcal{L}^{[\alpha]}}(\boldsymbol{r})$. Due to a corollary of the line bundle assumption, there is no tensor summation in the aforementioned equation. The correlation functions for the case of $\alpha = \beta$ were evaluated from DDD experiments [78] and were seen to decay at length scales similar to the spatial gradients of $\boldsymbol{\rho}^{[\alpha]}$. Incorporating these correlation-induced effects would still produce effects analogous to the 2D effective stresses (Eqs. (11)–(14)), but a local density approximation (as in Ref. [39]) would not be appropriate.

Because of the line bundle assumption that allows for such close analogy with the underlying discrete dislocation lines, many of the closure relations in the vector density formulation (e.g., correlation functions, reaction rate terms) are easily formulated in terms of statistics that can be gathered from DDD experiments [78,81–83]. However, this invites a possible accusation that the vector density dislocation dynamics are simply a numeric approximation to DDD by which nothing is gained. In practice, this is not the case. Before moving on, we would like to highlight several recent achievements of the vector density approach, which go beyond the capabilities of DDD.

Even in this line bundle regime, the dislocation density vector still describes the collective motion of dislocations. As a result, the mechanical fields that result can show the effect of their collective behavior. For instance, the antisymmetric portion of the deformation gradient demonstrates the rotation of the crystal lattice in different regions in the simulated domain. This lattice rotation field shows sudden changes in lattice direction in a single crystal, which are demarcated by regions of high dislocation content. This amounts to an observation of subgrain formation, and the regions of concentrated dislocation content correspond to the geometrically necessary boundaries and incidental dislocation boundaries observed in transmission electron microscopy experiments [84–86]. These structures, as well as other heterogeneities in the GND field, play a vital role in the context of recrystallization [87], while the formation of rotated subgrains has been linked to the onset of stage II hardening as new slip systems are activated [88]. Preliminary vector density dislocation dynamics studies have suggested that the emergence of dislocation patterns and subgrains is tied to the introduction of cross-slip and dislocation reactions [82,89]. Upon introduction of reaction terms, subgrain structures began to emerge (compared with Fig. 2) [89]. These capabilities of predicting the onset of subgrain formation will allow fruitful comparison with recent in situ methods for measuring the lattice rotations of subgrains [90]. Comparison between experiment and simulation will enable not only validation of the continuum model, but also will advance our understanding of the relationship between dislocation structures and the plastic response of metals.

In addition, it is worth noting that continuum dislocation dynamics models are capable of accounting for the kinematics of finite deformation [69,75,91,92]. We omit for present consideration of the numerous phenomenological crystal theories to focus on theories that explicitly consider the kinematics of dislocation densities. In this setting, the multiplicative decomposition of the deformation gradient is used to introduce elastic and plastic effects on the body (compared with the decomposition of the distortion field in Eqs. (20) and (21). These models all leverage the use of the Kröner–Nye dislocation density tensor, which Cermelli and Gurtin [93] showed to transform using Piola type transformations by analyzing Burgers circuits in both reference and deformed configurations. In FDM, the dislocation density tensor in the deformed configuration represents the dislocation system and closure relations are formed with this in mind. In the vector density approach, the dislocation density tensor is decomposed into slip system parts and either a scalar or vector density representation of dislocations are

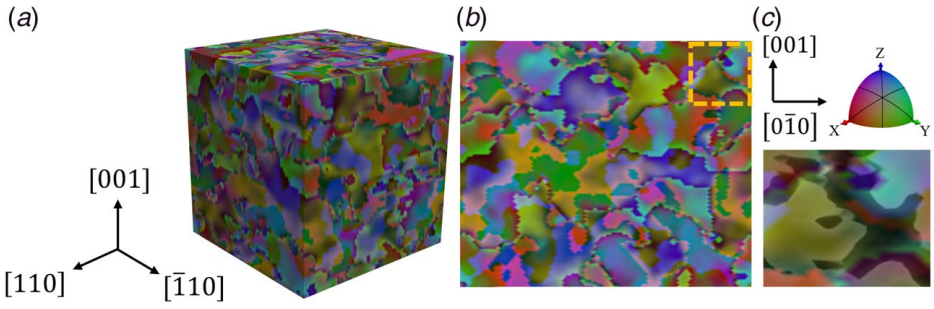

Fig. 2 Lattice rotations in a (5 × 5 × 5.3) μm^3 crystal volume of copper at 0.6% strain shown as an RGB plot where red, green, and blue correspond to the components of the normalized lattice rotation vector along [100], [010], and [001], respectively. Shown are the visualization of (*a*) the bulk, (*b*) slice along (100) plane, and (c) an enlarged portion of the (100) slice with the GND density distribution superposed (black) onto the lattice rotation fields.

formed. Hochrainer and Weger [75] derive the transport equations for the vector density in the intermediate configuration by decomposing the dislocation density tensor in the microstructure configuration into slip system components. Starkey et al. [91] derive not only the transport relations but also driving forces in both the deformed and reference configuration by using the two-point dislocation density tensors. Consistency between these two vector density models can be seen by taking the time derivative of the transformation relations between the referential and microstructure vector densities and plugging in the transport relations for the referential densities. In all these studies, the driving forces are obtained by examining the free-energy dissipation inequality for each of the corresponding configurations. This allows the corresponding Mandel stress to drive the dislocation motion in each configuration, and in some cases, an additional contribution to the driving force emerges from gradients of the free energy. Because the computational complexity of the vector density system does not scale with the total dislocation density and because the kinematics are preserved in the case of finite deformation, the vector density approach is not constrained to the small strain regime as is the case for DDD. Barring a breakdown of the line-bundle assumption at high strains, there does not seem to be an upper strain limit on the efficacy of vector density approaches. It is our opinion that in pushing dislocation dynamics to ever higher strains, vector density dislocation dynamics will emerge as a useful tool in describing microscopic plasticity.

5 Higher-Order Theories

As with the 2D models of dislocation motion, to be truly length-scale agnostic, the dislocation density measures must retain some information regarding the underlying dislocations' distribution over an orientation space [94]. First pioneered by Hochrainer and coworkers [80,95,96], considerable work has been done on the kinematics of curved line systems when this orientation distribution is taken into account. This presentation of the kinematics will follow most closely [97]. The formulation of these high-order kinematics of curved lines was motivated by the fact that without the line bundle constraint mentioned previously, the transport equation for the density field (29) cannot be expressed in terms of the density vector because the average slip rate vector is no longer proportional to the cross product of the average density and velocity fields, i.e.,

$$\left\langle \boldsymbol{v}^{[\alpha]} \times \boldsymbol{\rho}^{[\alpha]} \right\rangle \propto \left\langle \boldsymbol{v}^{[\alpha]} \right\rangle \times \left\langle \boldsymbol{\rho}^{[\alpha]} \right\rangle \tag{33}$$

To amend this issue, the dislocation density must be treated similarly to the 2D case: as a distribution not only over real space $\mathcal{M}$ but also over an orientation space $\mathbb{T}$, the unit circle parametrized by $\varphi = [0, 2\pi)$. This orientation space defines the line tangent $\hat{\boldsymbol{l}}(\varphi) := \cos(\varphi)\hat{\boldsymbol{b}} + \sin(\varphi)\hat{\boldsymbol{a}}$, where by $\hat{\boldsymbol{a}}$ we represent the positive edge dislocation direction $\hat{\boldsymbol{a}} := \hat{\boldsymbol{n}} \times \hat{\boldsymbol{b}}$. Rather than the ensemble average of space curves, the high-order density represents an ensemble average of "lifted curves," which are represented at every point by the tuple of not only their line direction $\boldsymbol{l}$ but also their curvature k, forming a four-vector $\boldsymbol{L}$, which moves according to the four-vector $\boldsymbol{V}$:

$$\boldsymbol{L}(\boldsymbol{r}, \varphi) := \left(\hat{\boldsymbol{l}}(\varphi), k(\boldsymbol{r}, \varphi)\right) \tag{34}$$

$$\boldsymbol{V}(\boldsymbol{r}, \varphi) := \left(v(\boldsymbol{r}, \varphi)\hat{\boldsymbol{l}}_{\perp}(\varphi), \vartheta(\boldsymbol{r}, \varphi)\right) \tag{35}$$

where $\hat{\boldsymbol{l}}_{\perp}(\varphi) := (\hat{\boldsymbol{l}}(\varphi) \times \hat{\boldsymbol{n}})$ and $\vartheta(\boldsymbol{r}, \varphi)$ are an orientation velocity, which captures the rotation of the lines. As opposed to the vector–density measure, which represents a spatial distribution times a line direction in real space, the high-order density also retains a component in the orientation space:

$$\boldsymbol{\rho}_{\mathrm{HO}}(\boldsymbol{r}, \varphi) := \rho(\boldsymbol{r}, \varphi)(\hat{\boldsymbol{l}}(\varphi), k(\boldsymbol{r}, \varphi)) \tag{36}$$

After the averaging process, note that the $k(\boldsymbol{r}, \varphi)$ represents the average curvature of all dislocation lines passing through $\boldsymbol{r}$, which have tangent direction $\hat{\boldsymbol{l}}(\varphi)$, and so the component of $\boldsymbol{\rho}_{\mathrm{HO}}^{[\alpha]}$ in the orientation "direction" is referred to as the curvature density $q(\boldsymbol{r}) := \rho(\boldsymbol{r}, \varphi)k(\boldsymbol{r}, \varphi)$. The key operation of this kinematic formulation is that the orientation velocity, ϑ, is expressible as the directional derivative of the real-space velocity, v, infourspace along $\boldsymbol{L}$:

$$\begin{aligned}\vartheta(\boldsymbol{r}, \varphi) &= \hat{\nabla}_{\boldsymbol{L}} v(\boldsymbol{r}, \varphi) \\ &= \left[\left(\hat{\boldsymbol{l}}(\varphi) \cdot \nabla\right) + k(\boldsymbol{r}, \varphi)\partial_{\varphi}\right] v(\boldsymbol{r}, \varphi)\end{aligned} \tag{37}$$

where $\hat{\nabla}$ represents the four-space gradient operator and ∇ represents the conventional gradient operator in the spatial dimensions.

The main result of this high-order dislocation density measure is that the evolution equation is expressible in terms of a single velocity field, even after ensemble averaging. This is expressed rather simply in terms of the four-space curl operator as follows:

$$\partial_t \boldsymbol{\rho}_{\mathrm{HO}} = -\mathrm{Curl}(\boldsymbol{V} \times \boldsymbol{\rho}_{\mathrm{HO}}) \tag{38}$$

Because of unintuitive nature of the high-dimensional differential operators, it is more simply expressed as two coupled evolution equations for the scalar dislocation density and the curvature density:

$$\partial_t \rho = -\left(\hat{\boldsymbol{l}}_{\perp} \cdot \nabla\right)(\rho v) - \partial_{\varphi}(\rho\vartheta) + qv \tag{39}$$

$$\partial_t q = \left(\hat{\boldsymbol{l}} \cdot \nabla\right)(\rho\vartheta) - \left(\hat{\boldsymbol{l}}_{\perp} \cdot \nabla\right)(qv) \tag{40}$$

These high-dimensional transport equations have been applied in the past to some simplified scenarios, notably a simplified micro-bending geometry [98,99], where they have been seen to generate hardening behavior in the tension and shear deformation of thin films [100]. However, there has been much interest in simplifying these evolution equations, as solutions of the high-dimensional transport equations require discretizing the orientation space at every point in the crystal. As a result, there have been efforts to create a reduced representation of the angular space. Early attempts at this simplification [101,102] began to integrate the dislocation density and curvature density over configuration space, but this process was formalized in [103]. This formulation recasts the evolution equations (39) and (40) as an infinite hierarchy of coupled equations by taking successive integral moments of the dislocation density tensor. These alignment tensors are expressed as follows:

$$\rho^{(0)}(\boldsymbol{r}) = \int d\varphi\, \rho(\boldsymbol{r}, \varphi) \tag{41}$$

$$\boldsymbol{\rho}^{(1)}(\boldsymbol{r}) = \int d\varphi\, \rho(\boldsymbol{r}, \varphi)\hat{\boldsymbol{l}}(\varphi) \tag{42}$$

$$\boldsymbol{\rho}^{(2)}(\boldsymbol{r}) = \int d\varphi\, \rho(\boldsymbol{r}, \varphi)\hat{\boldsymbol{l}}(\varphi) \otimes \hat{\boldsymbol{l}}(\varphi) \tag{43}$$

$$\boldsymbol{\rho}^{(n)}(\boldsymbol{r}) = \int d\varphi\, \rho(\boldsymbol{r}, \varphi)\hat{\boldsymbol{l}}(\varphi)^{\otimes n} \tag{44}$$

The zeroth and first alignment tensors represent the total and geometrically necessary dislocation content, respectively, at a point in the crystal. Their evolution equations are expressed as follows:

$$\partial_t \rho^{(0)} = \nabla \cdot \left(v\, \hat{\boldsymbol{n}} \times \boldsymbol{\rho}^{(1)}\right) + v\, \boldsymbol{Q}^{(0)} \tag{45}$$

$$\begin{aligned}\partial_t \boldsymbol{\rho}^{(n)} = \Big[&\nabla \times \left(v\, \hat{\boldsymbol{n}} \otimes \boldsymbol{\rho}^{(n-1)}\right) + (n-1)v\, \boldsymbol{Q}^{(n)} \\ &- (n-1)\left(\hat{\boldsymbol{n}} \times \boldsymbol{\rho}^{(n+1)}\right) \cdot \nabla v\Big]_{\mathrm{sym}}\end{aligned} \tag{46}$$

$$\partial_t q^{(0)} = \nabla \cdot \left(v\, \boldsymbol{Q}^{(1)} - \boldsymbol{\rho}^{(2)} \cdot \nabla v\right) \tag{47}$$

where $\boldsymbol{Q}^{(n)}$ are auxiliary curvature tensors of the form:

$$\boldsymbol{Q}^{(n)} = \int d\varphi \; q(\boldsymbol{r}, \varphi) \hat{\boldsymbol{l}}_{\perp}(\varphi) \otimes \hat{\boldsymbol{l}}_{\perp}(\varphi) \otimes \hat{\boldsymbol{l}}(\varphi)^{\otimes n-2} \tag{48}$$

These equations can be closed at order n if a sufficient form for $\boldsymbol{\rho}^{(n+1)}$ and $\boldsymbol{Q}^{(n)}$ in terms of lower order terms [97,104]. Comparisons to simplified DDD results showed closure at $n = 1$ (i.e., kinematics of the total and GND densities) to be insufficient to predict microstructure evolution [104,105] in some cases. Nonetheless, closure of the transport equations at first order seems to be the predominant usage [105–111].

There has been a significant work to compare these high-order kinematics of dislocations with DDD experiments [97,105,109,110,112]. These equations show excellent agreement in many problems regarding collections of expanding dislocation loops [97,105]. Moreover, many of the closure relations regarding the multipole expansion seem obtainable from DDD as tools emerge to collect curvature and orientation data from segment-based DDD experiments, especially when complemented by the advent of machine learning techniques [105,109,110].

Nonetheless, all of the aforementioned considerations have regarded only the kinematics of the system, with no regard to the kinetics. That is, they consider how the dislocation density measures move under a prescribed velocity field, they do not give a means of prescribing such a velocity field. The ubiquitous, zeroth-order kinetic strategy is to use some analogy of field dislocation mechanics to solve the long-range stress field resulting from the dislocation eigenstrain field [106,113] (compared with the mean-field stress in Eq. (11) or the self-consistent field formulation of Eq. (30)). However, more nuanced kinetics have been proposed. Hochrainer and coworkers have adapted the free-energy strategy of the 2D plastic potential to this 3D system, introducing back-stress-type driving forces as well as curvature-dependent driving forces, albeit in an in an ad hoc manner [114,115]. A rigorous coarse graining of the elastic energy functional [39] shows no dependence on the curvature density, but does support the introduction of back-stress terms, which have begun to be used in numerical implementations of high-order CDD [107]. With the exception of the long-range stress field, many of the kinetic effects depend on the dislocation correlation functions. In the high-dimensional CDD equations, the correlation functions are fully dependent on the angular coordinate. In the reduced representation, correlations between many combinations of the alignment tensors and their respective components must be considered [39]. As a result, correlation effects [39] have not been assessed quantitatively at present.

Moreover, while the kinematics are notable for being length-scale agnostic, this is somewhat of a hindrance for implementing dislocation reactions. Two theories have been developed to implement reactions, one due to Monavari and Zaiser [116] and another due to Sudmanns et al. [111]. Both involve enumerating possible reaction scenarios (e.g., glissile junctions, frank-read sources, double cross-slip) and implementing them individually. However, the heuristics by which source terms are derived differ significantly. In the implementation by Sudamanns et al. [111,112], reactions create sources of scalar density and curvature. Considering, for example, glissile junctions of type α formed by reacting systems β, γ :

$$\dot{\rho}_{\mathrm{gj}}^{[\alpha]} \propto \rho^{[\beta]} v^{[\beta]} \sqrt{\rho^{[\gamma]}} + \rho^{[\gamma]} v^{[\gamma]} \sqrt{\rho^{[\beta]}} \tag{49}$$

$$\dot{q}_{\mathrm{gj}}^{[\alpha]} \propto \mathrm{sgn}(v^{[\gamma]}) \dot{\rho}_{\mathrm{gj}}^{[\alpha]} \sqrt{\rho_t} \tag{50}$$

the difficulties of implementation become apparent. The orientation of the reagent slip systems have been seen to strongly affect glissile junction behavior [9], but this information is unavailable in the high-order equations, and homogenization arguments are needed to arrive at relevant reaction volumes dependent on the velocity fields and average dislocation spacings $1/\sqrt{\rho^{[\alpha]}}$. Models such as these show promise in introducing hardening behavior, but they require considerable statistical calibration from more finely resolved models [112].

In short, the higher order kinematics required to maintain a length-scale agnostic theory of continuum dislocation dynamics capture interesting and unforeseen consequences of the evolution of the average curvature of a dislocation system [100]. It represents a strong theory of the macroscopic effects of dislocation glide on plastic behavior. As the kinematic formulation has reached a simplified and tractable form, larger simulations have become feasible. Recent studies of the deformation of tricrystals [107], microwires [108], and early signs of pattern formation [106] demonstrate the utility of this descriptive framework. However, difficulties regarding incorporation of short-range interactions [114,115] as well as reaction processes [74,100,111,116,117] suggest that this will never be a suitable first-principles theory of dislocation motion at high strains.

6 Concluding Remarks

In this contribution, we have summarized several of the current models of continuum dislocation dynamics. We have seen the simplified 2D theory of dislocation motion, which, even if the physical system it considers is relevant only in specific bending geometries, is noteworthy in the fact that it points to the importance of statistical considerations in dislocation dynamics. Research into the 2D system is ongoing as increasingly nuanced statistical considerations reveal new interesting behavior. We examined field dislocation mechanics, which most closely follows the classical theory of distributed dislocations and is notable for its powerful description of internal mechanical fields and deformation kinematics. We considered the vector density approach to dislocation dynamics, which is commonly used by the present authors, with special emphasis on the implications of the line bundle assumption by which it treats only geometrically necessary dislocations. While this approach preserves more of the discrete line information than other continuum models due to its low-level treatment of the dislocation dynamics, several applications which go beyond the capabilities of DDD were discussed. Finally, we discussed the high-order theory of dislocation dynamics, which is capable of describing dislocation glide across all scales. Difficulties pertaining to the closure not only of the kinematics but also of the kinetics of the high-order dynamics were discussed; while it shows promise for being a physically based plasticity theory at large scales, it will always be reliant on lower level theories of dislocation motion.

Throughout, an emphasis has been placed on the role of DDD experiments in informing these continuum models. This is most often in the form of statistical information, which produces virtual effective stresses that enter in the kinetic closure of continuum theories. The 2D theories have the most straightforward relationship with DDD. Nonetheless, with a bit of statistical nuance, the vector density approach obtains these effective stresses, as well as closure relations for dislocation reactions. The high-order theory, as it requires homogenization arguments that have yet to be definitively determined, may require statistical considerations that rely on machine learning techniques to extract salient quantities from DDD.

In the course of this contribution, we have seen that many of these CDD frameworks are useful for treating different physical systems. These applications were discussed alongside each model, but we summarize them here. The 2D model of CDD is length-scale agnostic, but treats an overly simplified system of parallel edge dislocations. As a result, physical conclusions are restricted to certain specific loading configurations where the deformation is dominated by parallel edge dislocations. However, it remains a useful tool for studying the emergent properties, which arise from a statistical treatment of dislocation dynamics; this in turn can inform research into more general models pertaining to curved dislocations. The field dislocation

mechanics approach, modeling the dynamics of the total dislocation density tensor, is useful as a conceptual basis to modern phenomenological theories of plasticity. Its treatment of the mechanical fields caused by dislocations is useful in many applications and is a useful tool even in other frameworks where the evolution of the dislocation density is treated in a different manner. The vector density approach to dislocation dynamics holds only at low length scales due to the line bundle approximation, but it enables a robust treatment of the kinematics of finite deformation as well as dislocation reactions. These poise it uniquely to treat many interesting problems in microscopic plasticity at strains that go beyond the capabilities of discrete models. Finally, the high-order theory is—like the 2D theory—length-scale agnostic. As a result, it shows promise for creating a physically based theory of plasticity at higher scales. In fact, it has already been applied to consider simple polycrystals. However, due to the loss of spatial arrangement information at these higher scales, the high-order theory will always contain certain homogenization arguments that will represent an approximation of many of the microscopic dislocation processes that result in emergent behaviors in dislocation systems. As a result, it will always have to be informed by lower length-scale theories like DDD or the vector density approach.

As the field of dislocation dynamics progresses, it is the opinion of the present authors that the vector density approach and the high-order theory will become powerfully predictive physical theories of plasticity. They both will be useful in the simulation of different systems. This distinction will be rendered by the length scale of interest and by the resolution of the density field. As the resolution is made finer, the line bundle approximation renders the high-order field variables redundant; the key field variable becomes the GND density vector. The boundary of this transition—and as a result, the distinction between the two theories—is currently unclear. Future research into the valid regimes of the line bundle assumption will be needed to clearly demarcate the situations where these two theories should be applied.

Nonetheless, the outlook for the methods of continuum dislocation dynamics is compelling, to say the least. It seems poised to give us a physical basis for plasticity not only at micron-scales but also at the crystal level. As finite deformation methods for continuum dislocation dynamics have now emerged, an entirely new regime of strains now lie open to us. What new strengthening mechanisms might now be within our view? Which outstanding plasticity problems might now be put to rest? In the opinion of the present authors, continuum dislocation dynamics methods could represent a new frontier in plasticity research.

Acknowledgment

This work was supported by the US Department of Energy, Office of Science, Division of Materials Sciences and Engineering, through award number DE-SC0017718 and by the National Science Foundation, Division of Civil, Mechanical, and Manufacturing Innovation (CMMI), through Award No. 1663311 at Purdue University.

Conflict of Interest

The authors declare that they have no competing interests.

References

[1] Orowan, E., 1934, "Zur Kristallplastizität. I," Z. Phys., **89**(9–10), pp. 605–613.
[2] Polanyi, M., 1934, "Über Eine Art Gitterstörung, Die Einen Kristall Plastisch Machen Könnte," Z. Phys., **89**(9–10), pp. 660–664.
[3] Geoffrey Ingram Taylor, 1934, "The Mechanism of Plastic Deformation of Crystals. Part I—Theoretical," Proc. R. Soc. London. Seri. A, Cont. Papers Math. Phys. Charact., **145**(855), pp. 362–387.
[4] Arsenlis, A., Cai, W., Tang, M., Rhee, M, Oppelstrup, T., Hommes, G., Pierce, T. G., and Bulatov, V. V., 2007, "Enabling Strain Hardening Simulations With Dislocation Dynamics," Modell. Simul. Mater. Sci. Eng., **15**(6), pp. 553–595.
[5] Capolungo, L., and Taupin, V., 2019, "GD3: Generalized Discrete Defect Dynamics," Mater. Theory, **3**(1), pp. 1–21.
[6] Devincre, B., Madec, R., Monnet, G., Queyreau, S., Gatti, R., and Kubin, L., 2011, "Modeling Crystal Plasticity With Dislocation Dynamics Simulations: The "MicroMegas' Code," *Mechanics of Nano-Objects*, O. Thomas, A. Ponchet, and S. Forest, eds., ECOLE DES MINES, Paris, pp. 81–99.
[7] Ghoniem, N., Tong, S., and Sun, L., 2000, "Parametric Dislocation Dynamics: A Thermodynamics-Based Approach to Investigations of Mesoscopic Plastic Deformation," Phys. Rev. B - Condens. Matter Mater. Phys., **61**(2), pp. 913–927.
[8] Schwarz, K. W., 1999, "Simulation of Dislocations on the Mesoscopic Scale. I. Methods and Examples," J. Appl. Phys., **85**(1), pp. 108–119.
[9] Madec, R., Devincre, B., and Kubin, L. P., 2002, "On the Nature of Attractive Dislocation Crossed States," Comput. Mater. Sci., **23**(1), pp. 219–224.
[10] Devincre, B., Kubin, L. P., Lemarchand, C., and Madec, R., 2001, "Mesoscopic Simulations of Plastic Deformation," Mater. Sci. Eng. A., **309–310**, pp. 211–219.
[11] Hussein, A. M., Rao, S. I., Uchic, M. D., Dimiduk, D. M., and El-Awady, J. A., 2015, "Microstructurally Based Cross-Slip Mechanisms and Their Effects on Dislocation Microstructure Evolution in Fcc Crystals," Acta. Mater., **85**, pp. 180–190.
[12] Po, G., Cui, Y., Rivera, D., Cereceda, D., Swinburne, T. D., Marian, J., and Ghoniem, N., 2016, "A Phenomenological Dislocation Mobility Law for BCC Metals," Acta. Mater., **119**, pp. 123–135.
[13] Malka-Markovitz, A., Devincre, B., and Mordehai, D., 2021, "A Molecular Dynamics-Informed Probabilistic Cross-Slip Model in Discrete Dislocation Dynamics," Scr. Mater., **190**, pp. 7–11.
[14] Rhee, M., Zbib, H. M., Hirth, J. P., Huang, H., and De La Rubia, T., 1998, "Models for Long-/Short-Range Interactions and Cross Slip in 3D Dislocation Simulation of BCC Single Crystals," Modell. Simul. Mater. Sci. Eng., **6**(4), pp. 467–492.
[15] Shao, S., Abdolrahim, N., Bahr, D. F., Lin, G., and Zbib, H. M., 2014, "Stochastic Effects in Plasticity in Small Volumes," Int. J. Plast., **52**, pp. 117–132.
[16] Akarapu, S., Zbib, H. M., and Bahr, D. F., 2010, "Analysis of Heterogeneous Deformation and Dislocation Dynamics in Single Crystal Micropillars Under Compression," Int. J. Plast., **26**(2), pp. 239–257.
[17] Cui, Y., Po, G., and Ghoniem, N., 2016, "Controlling Strain Bursts and Avalanches at the Nano- to Micrometer Scale," Phys. Rev. Lett., **117**(15), p. 155502.
[18] Cui, Y., Po, G., and Ghoniem, N., 2017a, "Influence of Loading Control on Strain Bursts and Dislocation Avalanches at the Nanometer and Micrometer Scale," Phys. Rev. B, **95**(6), p. 064103.
[19] Sparks, G., Cui, Y., Po, G., Rizzardi, Q., Marian, J., and Maaß, R., 2019, "Avalanche Statistics and the Intermittent-to-Smooth Transition in Microplasticity," Phys. Rev. Mater., **3**(8), p. 080601.
[20] Crone, Joshua C., Munday, Lynn B., and Knap, J., 2015, "Capturing the Effects of Free Surfaces on Void Strengthening With Dislocation Dynamics," Acta. Mater., **101**, pp. 40–47.
[21] Khraishi, T. A., Zbib, H. M., Diaz De La Rubia, T., and Victoria, M., 2001, "Modelling of Irradiation-Induced Hardening in Metals Using Dislocation Dynamics," Philos. Mag. Lett., **81**(9), pp. 583–593.
[22] Cui, Y., Po, G., and Ghoniem, N., 2017, "Does Irradiation Enhance or Inhibit Strain Bursts at the Submicron Scale?," Acta. Mater., **132**, pp. 285–297.
[23] Zbib, H. M., Rhee, M., and Hirth, J. P., 1998, "On Plastic Deformation and the Dynamics of 3D Dislocations," Int. J. Mech. Sci., **40**(2–3), pp. 113–127.
[24] Sills, R. B., and Cai, W., 2014, "Efficient Time Integration in Dislocation Dynamics," Modell. Simul. Mater. Sci. Eng., **22**(2), p. 26.
[25] Sills, R. B., Aghaei, A., and Cai, W., 2016, "Advanced Time Integration Algorithms for Dislocation Dynamics Simulations of Work Hardening," Modell. Simul. Mater. Sci. Eng., **24**(4), p. 045019.
[26] Bertin, N., Aubry, S., Arsenlis, A., and Cai, W., 2019, "GPU-Accelerated Dislocation Dynamics Using Subcycling Time-Integration," Modell. Simul. Mater. Sci. Eng., **27**(7), p. 075014.
[27] Bertin, N., Upadhyay, M. V., Pradalier, C., and Capolungo, L., 2015, "A FFT-Based Formulation for Efficient Mechanical Fields Computation in Isotropic and Anisotropic Periodic Discrete Dislocation Dynamics," Modell. Simul. Mater. Sci. Eng., **23**(6), p. 065009.
[28] Deshpande, V. S., Needleman, A., and Van der Giessen, E., 2003, "Finite Strain Discrete Dislocation Plasticity," J. Mech. Phys. Solids., **51**, pp. 2057–2083.
[29] Irani, N., Remmers, J. J. C., and Deshpande, V. S., 2015, "Finite Strain Discrete Dislocation Plasticity in a Total Lagrangian Setting," J. Mech. Phys. Solids., **83**, pp. 160–178.
[30] El-Azab, A., 2000a, "Boundary Value Problem of Dislocation Dynamics," Modell. Simul. Mater. Sci. Eng., **8**(1), pp. 37–54.
[31] Wilkens, M., 1970, "The Determination of Density and Distribution of Dislocations in Deformed Single Crystals From Broadened X-Ray Diffraction Profiles," Phys. Status Solidi (A), **2**(2), pp. 359–370.
[32] Wilkens, M., 1970a, "Theoretical Aspects of Kinematical X-Ray Diffraction Profiles from Crystals Containing Dislocation Distributions," Fundamental Aspects of Dislocation Theory, Gaithersburg, MD, Apr. 21–25, Vol. 2, p. 715.
[33] Ungar, T., Mughrabi, H., Rönnpagel, D., and Wilkens, M., 1984, "X-ray Line-Broadening Study of the Dislocation Cell Structure in Deformed [001]-Orientated Copper Single Crystals," Acta. Metall., **32**(3), pp. 333–342.
[34] Groma, I., 1998, "X-ray Line Broadening Due to an Inhomogeneous Dislocation Distribution," Phys. Rev. B, **57**(13), pp. 7535–7542.

[35] Groma, I., 1997, "Link Between the Microscopic and Mesoscopic Length-Scale Description of the Collective Behavior of Dislocations," Phys. Rev. B, **56**(10), pp. 5807–5813.
[36] Groma, I., and Balogh, P., 1999, "Investigation of Dislocation Pattern Formation in a Two-Dimensional Self-Consistent Field Approximation," Acta. Mater., **47**(13), pp. 3647–3654.
[37] Zaiser, M., Miguel, M. C., and Groma, I., 2001, "Statistical Dynamics of Dislocation Systems: The Influence of Dislocation-Dislocation Correlations," Phys. Rev. B, **64**(22), p. 2241021.
[38] McQuarrie, D., 2000, *Statistical Mechanics*, University Science Books, Sausalito.
[39] Zaiser, M., 2015, "Local Density Approximation for the Energy Functional of Three-Dimensional Dislocation Systems," Phys. Rev. B, **92**(17), p. 174120.
[40] Groma, I., Csikor, F. F., and Zaiser, M., 2003, "Spatial Correlations and Higher-Order Gradient Terms in a Continuum Description of Dislocation Dynamics," Acta. Mater., **51**(5), pp. 1271–1281.
[41] Groma, I., Györgyi, G., and Kocsis, B., 2007, "Dynamics of Coarse Grained Dislocation Densities From an Effective Free Energy," Philosophical Magazine, **87**, pp. 1185–1199.
[42] Groma, I., Zaiser, M., and Ispánovity, P. D., 2016, "Dislocation Patterning in a Two-Dimensional Continuum Theory of Dislocations," Phys. Rev. B, **93**, p. 214110.
[43] Ispánovity, P. D., Papanikolaou, S., and Groma, I., 2020, "Emergence and Role of Dipolar Dislocation Patterns in Discrete and Continuum Formulations of Plasticity," Phys. Rev. B, **101**(2), p. 024105.
[44] Gulluoglu, A. N., Srolovitz, D. J., Lesar, R, and Lomdahl, P. S., 1988, "Dislocation Distributions in Two Dimensions," Scr. Metall., **23**, pp. 1347–1352.
[45] Wang, H. Y., Lesar, R, and Rickman, J. M., 1997, "Analysis of Dislocation Microstructures: Impact of Force Truncation and Slip Systems," Philos. Magaz. A, **78**(6), pp. 1195–1213.
[46] Groma, I., Györgyi, G., and Ispánovity, P. D., 2010, "Variational Approach in Dislocation Theory," Philos. Mag., **90**(27–28), pp. 3679–3695.
[47] Kooiman, M., Hütter, M., and Geers, M. G. D., 2015, "Effective Mobility of Dislocations From Systematic Coarse-Graining," J. Stat. Mech.: Theory. Exp., **2015**(6), p. P06005.
[48] Valdenaire, P.-L., Le Bouar, Y., Appolaire, B., and Finel, A., 2016, "Density-Based Crystal Plasticity: From the Discrete to the Continuum," Phys. Rev. B, **93**, p. 214111.
[49] Yefimov, S., Groma, István, and van der Giessen, E., 2004, "A Comparison of a Statistical-Mechanics Based Plasticity Model With Discrete Dislocation Plasticity Calculations," J. Mech. Phys. Solids., **52**(2), pp. 279–300.
[50] Schulz, K., Dickel, D., Schmitt, S., Sandfeld, S., Weygand, D., and Gumbsch, P., 2014, "Analysis of Dislocation Pile-Ups Using a Dislocation-Based Continuum Theory," Modell. Simul. Mater. Sci. Eng., **22**(2), p. 025008.
[51] Wu, R., Tüzes, D., Ispánovity, P. D., Groma, I., Hochrainer, T., and Zaiser, M., 2018, "Instability of Dislocation Fluxes in a Single Slip: Deterministic and Stochastic Models of Dislocation Patterning," Phys. Rev. B, **98**(5), p. 54110.
[52] Ispánovity, P. D., Tüzes, D., Szabó, P., Zaiser, M., and Groma, I., 2017, "Role of Weakest Links and System-Size Scaling in Multiscale Modeling of Stochastic Plasticity," Phys. Rev. B, **95**(5), p. 054108.
[53] Willis, J. R., 1967, "Second-Order Effects of Dislocations in Anisotropic Crystals," Int. J. Eng. Sci., **5**(2), pp. 171–190.
[54] Nye, J. F., 1953, "Some Geometrical Relations in Dislocated Crystals," Acta. Metall., **1**(2), pp. 153–162.
[55] Gurtin, M. E., 2000, "On the Plasticity of Single Crystals: Free Energy, Microforces, Plastic-Strain Gradients," J. Mech. Phys. Solids., **48**(5), pp. 989–1036.
[56] Shizawa, K., and Zbib, H. M., 1999, "A Thermodynamical Theory of Plastic Spin and Internal Stress With Dislocation Density Tensor," J. Eng. Mater. Technol., Trans. ASME, **121**(2), pp. 247–253.
[57] Shizawa, K., and Zbib, H. M., 1999, "A Thermodynamical Theory of Gradient Elastoplasticity With Dislocation Density Tensor. I: Fundamentals," Int. J. Plast., **15**(9), pp. 899–938.
[58] Shizawa, K., Kikuchi, K., and Zbib, H. M., 2001, "A Strain-Gradient Thermodynamic Theory of Plasticity Based on Dislocation Density and Incompatibility Tensors," Mater. Sci. Eng. A., **309–310**, pp. 416–419.
[59] Acharya, A., 2001, "A Model of Crystal Plasticity Based on the Theory of Continuously Distributed Dislocations," J. Mech. Phys. Solids., **49**(4), pp. 761–784.
[60] Roy, A., and Acharya, A., 2006, "Size Effects and Idealized Dislocation Microstructure at Small Scales: Predictions of a Phenomenological Model of Mesoscopic Field Dislocation Mechanics: Part II," J. Mech. Phys. Solids., **54**(8), pp. 1711–1743.
[61] Acharya, A., and Roy, A., 2006, "Size Effects and Idealized Dislocation Microstructure at Small Scales: Predictions of a Phenomenological Model of Mesoscopic Field Dislocation Mechanics: Part I," J. Mech. Phys. Solids., **54**(8), pp. 1687–1710.
[62] Mura, T., 1963, "Continuous Distribution of Moving Dislocations," Philos. Mag., **8**(89), pp. 843–857.
[63] Kosevich, A. M., 1965, "Dynamical Theory of Dislocations," Soviet Phys. Uspekhi, **7**(6), pp. 837–854.
[64] Acharya, A., 2004, "Constitutive Analysis of Finite Deformation Field Dislocation Mechanics," J. Mech. Phys. Solids., **52**(2), pp. 301–316.
[65] Lin, P., Vivekanandan, V., Starkey, K., Anglin, B., Geller, C., and El-Azab, A., 2021, "On the Computational Solution of Vector-Density Based Continuum Dislocation Dynamics Models: A Comparison of Two Plastic Distortion and Stress Update Algorithms," Int. J. Plast., **138**, p. 102943.
[66] Acharya, A., 2003, "Driving Forces and Boundary Conditions in Continuum Dislocation Mechanics," Proc. R. Soc. A: Math., Phys. Eng. Sci, **459**(2034), pp. 1343–1363.
[67] Brenner, R., Beaudoin, A. J., Suquet, P., and Acharya, A., 2014, "Numerical Implementation of Static Field Dislocation Mechanics Theory for Periodic Media," Philos. Mag., **94**(16), pp. 1764–1787.
[68] Puri, S., Das, A., and Acharya, A., 2011, "Mechanical Response of Multicrystalline Thin Films in Mesoscale Field Dislocation Mechanics," J. Mech. Phys. Solids., **59**(11), pp. 2400–2417.
[69] Arora, R., and Acharya, A., 2020, "Dislocation Pattern Formation in Finite Deformation Crystal Plasticity," Int. J. Solids. Struct., **184**, pp. 114–135.
[70] Morin, L., Brenner, R., and Suquet, P., 2019, "Numerical Simulation of Model Problems in Plasticity Based on Field Dislocation Mechanics," Modell. Simul. Mater. Sci. Eng., **27**(8), p. 085012.
[71] Bertin, N., and Capolungo, L., 2018, "A FFT-Based Formulation for Discrete Dislocation Dynamics in Heterogeneous Media," J. Comput. Phys., **355**, pp. 366–384.
[72] Kröner, E., 2001, "Benefits and Shortcomings of the Continuous Theory of Dislocations," Int. J. Solids. Struct., **38**(6–7), pp. 1115–1134.
[73] El-Azab, A., and Po, G., 2018, "Continuum Dislocation Dynamics: Classical Theory and Contemporary Models," *Handbook of Materials Modeling*, W. Andreoni, and S. Yip, eds., Springer International Publishing, Cham, pp. 1–25.
[74] Weger, B., and Hochrainer, T., 2019, "Leaving the Slip System–Cross Slip in Continuum Dislocation Dynamics," PAMM, **19**(1), p. 201900441.
[75] Hochrainer, T., and Weger, B., 2020, "Is Crystal Plasticity Non-Conservative? Lessons From Large Deformation Continuum Dislocation Theory," J. Mech. Phys. Solids., **141**, p. 103957.
[76] Xia, S. X., and El-Azab, A, 2015, "A Preliminary Investigation of Dislocation Cell Structure Formation in Metals Using Continuum Dislocation Dynamics," IOP Conference Series: Materials Science and Engineering, **89**, p. 012053.
[77] Xia, S. X., and El-Azab, A., 2015, "Computational Modelling of Mesoscale Dislocation Patterning and Plastic Deformation of Single Crystals," Modell. Simul. Mater. Sci. Eng., **23**, p. 055009.
[78] Anderson, J. P., and El-Azab, A., 2021, "On the Three-Dimensional Spatial Correlations of Curved Dislocation Systems," Materials Theory, **5**, p. 1. https://arxiv.org/abs/2006.11142.
[79] Xia, S. X., 2016, "Continuum Dislocation Dynamics Modelling of the Deformation of FCC Single Crystals," Ph.d. thesis, Purdue University.
[80] Hochrainer, T., Zaiser, M., and Gumbsch, P., 2007, "A Three-Dimensional Continuum Theory of Dislocation Systems: Kinematics and Mean-Field Formulation," Philos. Mag., **87**(8–9), pp. 1261–1282.
[81] Lin, P., and El-Azab, A., 2020, "Implementation of Annihilation and Junction Reactions in Vector Density-Based Continuum Dislocation Dynamics," Modell. Simul. Mater. Sci. Eng., **28**(4), p. 045003.
[82] Xia, S., Belak, J., and Anter El-Azab, 2016, "The Discrete-Continuum Connection in Dislocation Dynamics: I. Time Coarse Graining of Cross Slip," Modell. Simul. Mater. Sci. Eng., **24**(7), p. 075007.
[83] Deng, J., and El-Azab, A., 2010, "Temporal Statistics and Coarse Graining of Dislocation Ensembles," Philosophical Magazine, **90**, pp. 3651–3678.
[84] Godfrey, A., and Hughes, D. A., 2000, "Scaling of the Spacing of Deformation Induced Dislocation Boundaries," Acta. Mater., **48**(8), pp. 1897–1905.
[85] Hughes, Darcy A., Liu, Q., Chrzan, D. C., and Hansen, N., 1997, "Scaling of Microstructural Parameters: Misorientations of Deformation Induced Boundaries," Acta. Mater., **45**(1), pp. 105–112.
[86] Hughes, D. A., Hansen, N., and Bammann, D. J., 2003, "Geometrically Necessary Boundaries, Incidental Dislocation Boundaries and Geometrically Necessary Dislocations," Scr. Mater., **48**(2), pp. 147–153.
[87] Humphreys, F. J., and Hatherly, M., 2012, *Recrystallization and Related Annealing Phenomena*, 2nd ed., Elsevier, Oxford, UK.
[88] Hull, D., and Bacon, D. J., 2011, "Chapter 10—Strength of Crystalline Solids," Hull, D., and Bacon, D. J., eds., *Introduction to Dislocations*, 5th. ed., Butterworth-Heinemann, Oxford, pp. 205–249.
[89] Vivekanandan, V., Lin, P., Winther, G., and El-Azab, A., 2021, "On the Implementation of Dislocation Reactions in Continuum Dislocation Dynamics Modeling of Mesoscale Plasticity," J. Mech. Phys. Solids., **149**, p. 104327.
[90] Juul, N. Y., Oddershede, J., and Winther, G., 2020, "Analysis of Grain-Resolved Data From Three-Dimensional X-Ray Diffraction Microscopy in the Elastic and Plastic Regimes," JOM, **72**(1), pp. 83–90.
[91] Starkey, K., Winther, G., and El-Azab, A., 2020, "Theoretical Development of Continuum Dislocation Dynamics for Finite-Deformation Crystal Plasticity at the Mesoscale," J. Mech. Phys. Solids., **139**, p. 103926.
[92] Po, G., Huang, Y., and Ghoniem, N., 2019, "A Continuum Dislocation-Based Model of Wedge Microindentation of Single Crystals," Int. J. Plast., **114**, pp. 72–86.
[93] Cermelli, P., and Gurtin, M. E., 2001, "On the Characterization of Geometrically Necessary Dislocations in Finite Plasticity," J. Mech. Phys. Solids., **49**(7), pp. 1539–1568.
[94] El-Azab, A., 2000, "Statistical Mechanics Treatment of the Evolution of Dislocation Distributions in Single Crystals," Phys. Rev. B, **61**(18), pp. 11956–11966.
[95] Hochrainer, T., 2007, "Evolving Systems of Curved Dislocations: Mathematical Foundations of a Statistical Theory," Ph.D. thesis, Karlsruhe Institute of Technology.
[96] Hochrainer, T., Sandfeld, S., Zaiser, M., and Gumbsch, P., 2014, "Continuum Dislocation Dynamics: Towards a Physical Theory of Crystal Plasticity," J. Mech. Phys. Solids., **63**, pp. 167–178.

[97] Monavari, M., Zaiser, M., and Sandfeld, S., 2014, "Comparison of Closure Approximations for Continuous Dislocation Dynamics," Mater. Res. Soc. Symp. Proc., **1651**, p. 302.
[98] Sandfeld, S., Hochrainer, T., Gumbsch, P., and Zaiser, M., 2010, "Numerical Implementation of a 3D Continuum Theory of Dislocation Dynamics and Application to Micro-Bending," Philos. Mag., **90**(27–28), pp. 3697–3728.
[99] Sandfeld, S., 2010, "The Evolution of Dislocation Density in a Higher-Order Continuum Theory of Dislocation Plasticity," Ph.D. thesis, University of Edinburgh.
[100] Sandfeld, S., Thawinan, E., and Wieners, C., 2015, "A Link Between Microstructure Evolution and Macroscopic Response in Elasto-Plasticity: Formulation and Numerical Approximation of the Higher-Dimensional Continuum Dislocation Dynamics Theory," Int. J. Plast., **72**, pp. 1–20.
[101] Sandfeld, S., Hochrainer, T., Zaiser, M., and Gumbsch, P., 2011, "Continuum Modeling of Dislocation Plasticity: Theory, Numerical Implementation, and Validation by Discrete Dislocation Simulations," J. Mater. Res., **26**(5), pp. 623–632.
[102] Hochrainer, T., Zaiser, M., and Gumbsch, P., 2010, "Dislocation Transport and Line Length Increase in Averaged Descriptions of Dislocations," AIP. Conf. Proc., **1168**, pp. 1133–1136.
[103] Hochrainer, T., 2015, "Multipole Expansion of Continuum Dislocations Dynamics in Terms of Alignment Tensors," Philos. Mag., **95**(12), pp. 1321–1367.
[104] Monavari, M., Sandfeld, S., and Zaiser, M., 2016, "Continuum Representation of Systems of Dislocation Lines: A General Method for Deriving Closed-Form Evolution Equations," J. Mech. Phys. Solids., **95**, pp. 575–601.
[105] Sandfeld, S., and Po, G., 2015, "Microstructural Comparison of the Kinematics of Discrete and Continuum Dislocations Models," Modell. Simul. Mater. Sci. Eng., **23**(8), p. 085003.
[106] Sandfeld, S., and Zaiser, M., 2015, "Pattern Formation in a Minimal Model of Continuum Dislocation Plasticity," Modell. Simul. Mater. Sci. Eng., **23**(6), p. 065005.
[107] Schulz, K., Wagner, L., and Wieners, C., 2019, "A Mesoscale Continuum Approach of Dislocation Dynamics and the Approximation by a Runge-Kutta Discontinuous Galerkin Method," Int. J. Plast., **120**, pp. 248–261.
[108] Zoller, K., and Schulz, K., 2020, "Analysis of Single Crystalline Microwires Under Torsion Using a Dislocation-Based Continuum Formulation," Acta. Mater., **191**, pp. 198–210.
[109] Song, H., Gunkelmann, N., Po, G., and Sandfeld, S., 2021, "Data-Mining of Dislocation Microstructures: Concepts for Coarse-Graining of Internal Energies," Modell. Simul. Mater. Sci. Eng., **29**, p. 035005.
[110] Steinberger, D., Gatti, R., and Sandfeld, S., 2016, "A Universal Approach Towards Computational Characterization of Dislocation Microstructure," JOM, **68**(8), pp. 2065–2072.
[111] Sudmanns, M., Stricker, M., Weygand, D., Hochrainer, T., and Schulz, K., 2019, "Dislocation Multiplication by Cross-Slip and Glissile Reaction in a Dislocation Based Continuum Formulation of Crystal Plasticity," J. Mech. Phys. Solids., **132**, p. 103695.
[112] Sudmanns, M., Bach, J., Weygand, D., and Schulz, K., 2020, "Data-driven Exploration and Continuum Modeling of Dislocation Networks," Modell. Simul. Mater. Sci. Eng., **28**(6), p. 065001.
[113] Sandfeld, S., Monavari, M., and Zaiser, M., 2013, "From Systems of Discrete Dislocations to a Continuous Field Description: Stresses and Averaging Aspects," Modell. Simul. Mater. Sci. Eng., **21**(8), p. 085006.
[114] Hochrainer, T., 2016, "Thermodynamically Consistent Continuum Dislocation Dynamics," J. Mech. Phys. Solids., **88**, pp. 12–22.
[115] Groma, I., Ispánovity, P. D., and Hochrainer, T., 2021, "Dynamics of Curved Dislocation Ensembles," Phys. Rev., **103**, p. 174101.
[116] Monavari, M., and Zaiser, M., 2018, "Annihilation and Sources in Continuum Dislocation Dynamics," Mater. Theory, **2**(1), p. 3.
[117] Stricker, M., Sudmanns, M., Schulz, K., Hochrainer, T., and Weygand, D., 2018, "Dislocation Multiplication in Stage II Deformation of FCC Multi-Slip Single Crystals," J. Mech. Phys. Solids., **119**, pp. 319–333.